Diffusion- and Reaction-Limited Growth of Carbon Nanotube Forests

Christoph Tobias Wirth,* Can Zhang, Guofang Zhong, Stephan Hofmann, and John Robertson

Department of Engineering, University of Cambridge, Cambridge CB2 1PZ, U.K.

ABSTRACT We present a systematic study of the temperature and pressure dependence of the growth rate of vertically aligned small diameter (single- and few-walled) carbon nanotube forests grown by thermal chemical vapor deposition over the temperature range 560—800 °C and 10^{-5} to 14 mbar partial pressure range, using acetylene as the feedstock and Al_2O_3-supported Fe nanoparticles as the catalyst. We observe a pressure dependence of $P^{0.6}$ and activation energies of <1 eV. We interpret this as a growth rate limited by carbon diffusion in the catalyst, preceded by a pre-equilibrium of acetylene dissociation on the catalyst surface. The carbon nanotube forest growth was recorded by high-resolution real-time optical imaging.

The growth of carbon nanotubes by catalytic chemical vapor deposition (CVD) is of great interest for applications such as composites, conducting composites, transparent electrodes[1-3] and for interconnects, supercapacitor electrodes, thermal management films, microelectromechanical systems (MEMS), adhesive layers, and yarns.[4-8] The latter applications require the controlled, surface-bound growth of high-density vertically aligned forests or "mats" of multi-walled[9-12] or single-walled nanotubes.[13-17] For these reasons, it is of great importance to understand which processes control the growth rate, which factors lead to high efficiency growth, and which factors cause the growth rate to slow down or stop.[18-23] The CVD growth rate can be limited by diffusion and mass transfer in the gas phase,[22,23] surface reactions on the catalyst, or carbon diffusion through the catalyst bulk[24-27] or over the catalyst surface,[28-30] as shown schematically in Figure 1. For many years, from the initial observations on carbon nanofibers to recent analysis of single-walled nanotubes (SWNTs), it was generally assumed that carbon diffusion through or over the catalyst nanoparticle was the rate-limiting step.[24,26-31] However, if carbon diffusion through a metal nanoparticle was the

only factor, this would not explain the importance of the catalyst quality and the type of feedstock. Here, we present data on the pressure and temperature dependence of the growth rate, which indicates that the mechanism is more complex and includes both a molecular dissociation step and a diffusion step.

The ability to grow macroscopically sized mats of nanotubes means that we can now measure growth kinetics by real-time imaging techniques,[32-36] rather than relying on postgrowth analysis of many samples by *ex situ* methods such as scanning electron microscopy (SEM). Here we use *in situ* optical imaging, calibrated and supplemented by *ex situ* SEM measurements, to measure the growth rate of small (1—4 nm) diameter nanotube mats, for the case of Fe catalyst on an Al_2O_3 support[33] and acetylene as feedstock.

Growth is carried out on Si(100) wafer covered with 200 nm of thermal SiO_2, itself covered with a 10 nm thick Al_2O_3 layer formed by sputter deposition. Onto this is deposited a 0.5—1 nm thick Fe film at ~1 Å/s at a base pressure of under 10^{-6} mbar. The film thickness was monitored *in situ* by a quartz crystal microbalance and calibrated *ex situ* by atomic force microscopy (AFM, Veeco Explorer) and spectroscopic ellipsometry (Woollam, M-2000 V).

Depending on the growth pressure, the catalyst-coated Si substrates are then transferred to the respective growth systems. Figure 2a—f shows SEM images (tilted view) of the forests grown at different temperatures and pressures. These views show the side of a forest plus the top of the forests with their entangled tubes. The nanotube length is taken as the forest height. For the case of CVD at 10^{-5} mbar, the nanotube forest has only just evolved from an entangled

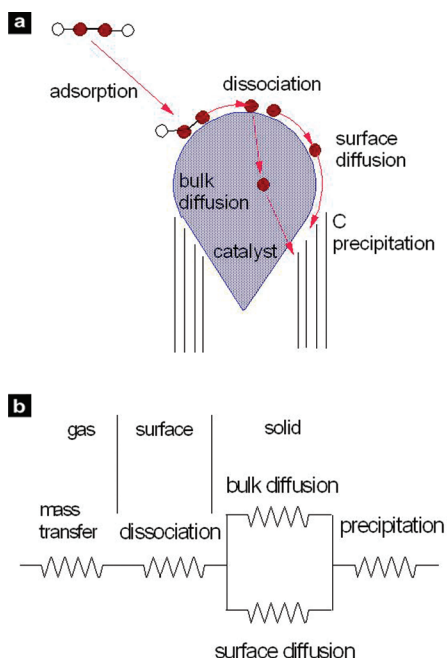*Address correspondence to ctw31@cam.ac.uk.

Figure 1. (a) Schematic of CNT growth process. (b) Schematic of possible rate-limiting processes.

network. The growth rate is taken from the initial growth rate.

Atmospheric pressure CVD is performed in a conventional 2" quartz tube furnace (Carbolite). Vertically aligned carbon nanotube arrays are grown for 5 min in a temperature range of 560−800 °C in 200:500:10 sccm $Ar/H_2/C_2H_2$ mixtures at a C_2H_2 partial pressure of 10−14 mbar. The reaction temperature is ramped at 20 °C/min in Ar flow. This is called the hot-wall system.

For real-time optical imaging, a custom-built direct heater is loaded into the quartz tube (cold-wall conditions) where the 5×15 mm^2 catalyst-coated substrate is clamped between two copper posts and is resistively heated in the same reactant mixture. The stripe is heated to ~750 °C at its center within 5−10 s of applying the power. The temperature is maintained by a DC current and is monitored by a pyrometer which is calibrated against a thermocouple. This system allows very rapid heating because only the substrate itself is heated, not the whole furnace. The growth was monitored for 30 min by a digital camera mounted normal to the quartz tube. Movies of the growth process compiled of the images taken every 2 s are given in the Supporting Information. Figure 2g shows a temperature profile for the directly

heated substrates and an image of the grown nanotube mats. The catalyst is patterned to make the height measurements easier and to allow temperature measurements at each spot. Nanotube lengths are taken as forest heights. Figure 2h shows the evolution of mat height with time. A slightly sublinear growth regime is seen, but we do not see the abrupt growth termination seen by some groups.[19,20,34]

The lower pressure growth was carried out in a stainless steel growth chamber previously used for plasma-enhanced CVD on resistively heated substrates,[28] but here *without* plasma ignition. For low pressure growth ($10^{-3}-10^{-2}$ mbar acetylene), the catalyst was activated by heating in 0.5 mbar ammonia.[37] Growth was initiated when C_2H_2 was introduced into the previously evacuated chamber. Growth in the range of 10^{-1} mbar C_2H_2 partial pressure was performed in a H_2/C_2H_2 mixture at a total pressure of 15 mbar. In this case, the catalyst was heated in H_2 prior to growth.

Using the rapid heating cold-wall method, a forest height of about 1 mm is reached after 5 min whereas a furnace run with hot-wall conditions at the same temperature of 750 °C yields only 100 μm. The average MWNT diameter is 5 nm with a density of ~10^{12} CNTs/cm^2. There is less catalyst sintering for the fast heating case.

The resulting carbon nanostructures were analyzed by SEM (Jeol 6340 and LEO 1530 VP FEGSEM), high-resolution transmission electron microscopy (HRTEM, Jeol JEM 4000EX, 400 kV),[8,38,39] and multi-wavelength Raman spectroscopy (Renishaw).[8,22,37]

The nanotubes are single-walled at subatmospheric pressure but are small diameter multi-walled nanotubes (MWNTs) when grown at atmospheric pressure. The
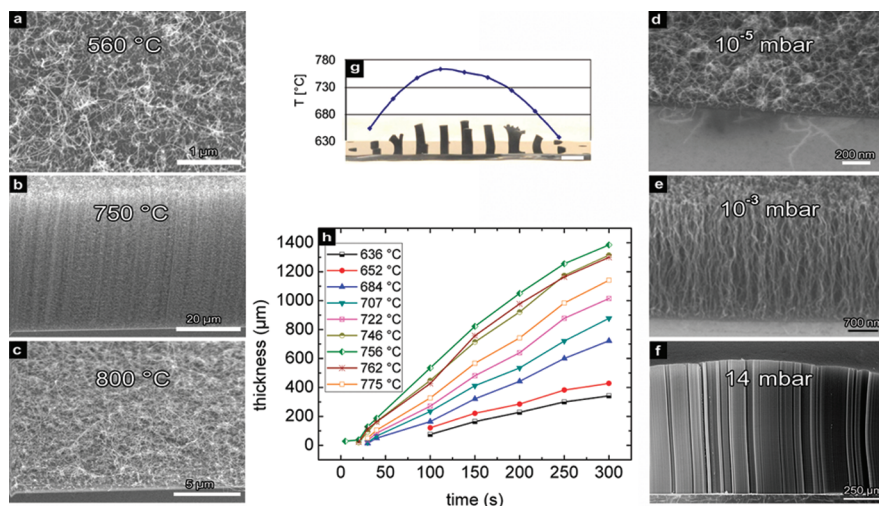

Figure 2. (a−c) SEM images of CNT growth from Al_2O_3-supported Fe films performed in 200:500:10 sccm $Ar/H_2/C_2H_2$ at atmospheric pressure for 5 min at different temperatures. (d−f) SEM images of CNTs grown for 5 min at ~700 °C at different C_2H_2 partial pressures: (d) growth at 10^{-5} mbar. The Fe film was annealed in UHV for 5 min. (e) CVD at 2.5×10^{-3} mbar. The catalyst was first annealed in NH$_3$ for 5 min. (f) Atmospheric pressure CVD with direct heating method. (g) Temperature profile across the resistively heated sample. The Si substrate shows an approximately Gaussian temperature profile centered at ~750 °C. Scale bar: 2 mm. (h) Length of CNT arrays *versus* time obtained by optical real-time imaging.
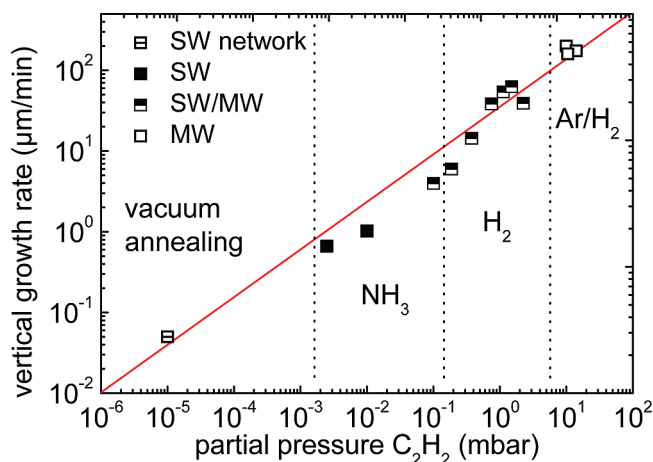
Figure 3. C_2H_2 partial pressure dependence of CNT growth rate in cold-wall conditions, $P^{0.61\pm0.03}$. CNTs were grown from an Fe/Al_2O_3 catalyst at 700 °C for 5 min. For low pressures, the growth gas is pure acetylene, and the Fe film was activated in an NH_3 atmosphere. For the higher pressure regime, growth was performed in a H_2 mixture and above 10 mbar in an Ar/H_2 mixture.

SWNTs have a diameter from 0.8 to 2.2 nm from HR-TEM and show the radial breathing modes with a wide range of chiralities, and in this sense, they are similar to those grown by water-assisted CVD.[14] The catalyst particle sizes were previously characterized by AFM, and it is found that the nanotube diameter closely reflects the catalyst particle diameter size distribution.[33,37,40,41]

To understand the growth process, we first studied the pressure dependence over a wide range using acetylene as feedstock. Figure 3 shows the pressure dependence of the initial growth rate. We find that the growth rate varies with acetylene partial pressure P as $P^{0.61\pm0.03}$ over 7 orders of magnitude of pressure. This is a very wide pressure range. An explicit pressure dependence cannot be reconciled with a simple diffusion-limited process, which would be independent of pressure, and we return to this later.

The temperature dependence of growth rate was measured over a C_2H_2 partial pressure range of 4 orders of magnitude, 14 mbar at atmospheric pressure, 10^{-1} mbar at 15 mbar total pressure, and 10^{-3} mbar partial pressure. Figure 4a shows an Arrhenius plot of the temperature dependence of linear growth rate for the atmospheric pressure case. An activation energy of 0.95 eV is found for hot-wall furnace growth and 0.92 eV for the directly heated cold-wall case. Figure 4b,c shows the temperature dependence at the pressure of 10^{-1} and 10^{-3} mbar. The activation energies are found to be quite similar, 0.93 and 0.98 eV, respectively. The fact that the activation energy is sizable and similar at these different pressures indicates that the mechanism is in the same regime, and that, in particular for high pressures, it has not passed into a mass-transfer-limited CVD regime which is characterized by a low activation energy. The fall off in growth at high temperature might be due to a deactivation of catalyst by carburization[21] or sintering.[42]

We now consider the mechanism. First, we note that nanotube growth is a heterogeneous catalytic process, whose efficiency varies widely. A reaction yield (strictly, a catalyst efficiency) has been defined as the weight of nanotubes produced divided by the weight of catalyst used,[14] and this varies from 0.1 to factors of over 10^4 in the present work[22] and in the water-assisted growth.[14] The yield depends on the precise activation state of the catalyst, and this might not be independent of pressure and temperature in our experiments. Thus, the error bars on our data are high, and this is why we studied the kinetics over a large range of pressures.

The previous discussion of growth mechanisms of carbon nanotubes has tended to focus on a diffusion-limited mechanism, whether bulk or surface diffusion. The first experiments of Baker et al.[24] on carbon nanofibers identified carbon diffusion through the catalyst bulk as the rate-limiting step, based on the similarity of the activation energy of growth and carbon diffusion.[43] Rostrup-Nielsen et al.[25] and Klinke et al.[26] noted that concentration gradients rather than thermal gradients drove growth. The catalyst is generally solid,[39] so the diffusion energy is sizable in comparison to a liquid state.[31] Chhowalla et al.[27] also suggested that MWNT growth by PECVD was bulk-diffusion-limited, based on the activation energy of 1.4 eV, and that the growth rate varied inversely with catalyst particle diameter.[40] Subsequently, some groups reported higher activation energies over a limited temperature range, without commenting too much on the underlying mechanism. For example, Puretzky et al.[18] observed a high activation energy of ~2.4 eV, Vinten et al.[44] reported 2.3 eV using ethanol as precursor, and Zhu et al.[45] reported an activation energy of 2.2 eV over a narrow temperature range. On the other hand, Lee et al.[46] and Kim et al.[47] reported activation energies of order 1.3 eV. Liu et al.[31] reported an activation energy of 1.6 eV, with acetylene as precursor. Then Hofmann et al.[28] reported a very low activation energy of 0.25 eV for PECVD growth, which they attributed to the plasma dissociation of the feedstock and surface diffusion-limited growth. A few cases of gas phase diffusion-limited CVD have been seen. Zhong et al.[22] and Noda et al.[48] observed a parabolic growth law, plus increased growth at regions of better gas access, which suggested that a gas phase limit could occur due to the narrow intertube spacing in the highest density forests. Xiang et al.[23] analyzed whether growth rate decreases were arising from the Knudsen diffusion through the growing forest or catalyst deactivation. (Note, however, that a Knudsen limited regime would have a weaker temperature dependence than we find.)

Here, we propose that a $P^{0.5}$ dependence can be explained by a combination of dissociative adsorption of acetylene on the catalyst surface followed by a rate-limiting step of solid-state diffusion. The acetylene adsorbs on the catalyst surface

$$C_2H_{2\ gas} \rightleftharpoons C_2H_{2\ ads}$$
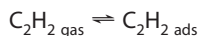
and it then dissociates into adsorbed carbon atoms

$$C_2H_{2\ ads} \rightleftharpoons 2C_{ads} + H_2 \qquad (1)$$
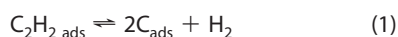
We assume that this reaction consists of two rate constants for forward and backward reactions

$$R_1 = k_1[C_2H_2]$$

$$R_{-1} = k_{-1}[C_{ads}]^2[H_2]$$

These reactions are followed by a slower reaction of carbon diffusing through solid catalyst and precipitating to form the nanotube

$$C_{ads} \rightarrow C_{CNT} \qquad (2)$$

which is given by the rate

$$R_{CNT} = k_2[C_{ads}]$$

If $k_{-1} \gg k_2$, then this is equivalent to a pre-equilibrium of dissociated carbon atoms governed by an equilibrium constant K
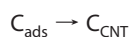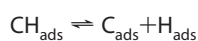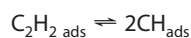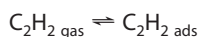
$$K = \frac{k_1}{k_{-1}} = \frac{[C_{ads}]^2[H_2]}{[C_2H_2]} \qquad (3)$$

followed by the slower reaction 2. The overall rate is proportional to the concentration, [C], or from eq 3, it is proportional to the [C$_2$H$_2$] concentration to the power 1/2

$$R_{CNT} = k_2[C_{ads}] \sim k_2K'^{1/2}[C_2H_2]^{1/2} \qquad (4)$$

where [H$_2$] has been absorbed into K'.

There are a number of possible elementary reaction schemes for these reactions. One possibility is

$$C_2H_{2\ gas} \rightleftharpoons C_2H_{2\ ads}$$

$$C_2H_{2\ ads} \rightleftharpoons 2CH_{ads}$$

$$CH_{ads} \rightleftharpoons C_{ads} + H_{ads}$$

$$2H_{ads} \rightarrow H_{2\ gas} \qquad (5)$$

$$C_{ads} \rightarrow C_{CNT}$$

with eq 5 being an exothermic evolution. In this case, the [H$_2$] does not enter the pre-equilibrium step. In the linear growth regime, where the catalyst is highly active, we approximate the catalyst by a nearly empty surface, that is, assume the fractional coverage by adsorbates to be negligible. Note that Pirard et al.[49] found a reaction order of zero for hydrogen, for ethylene as precursor.

Figure 5 shows schematically the energy diagram of the three processes. The overall experimental activation energy corresponds to the energy of the diffusion transition state above that of acetylene

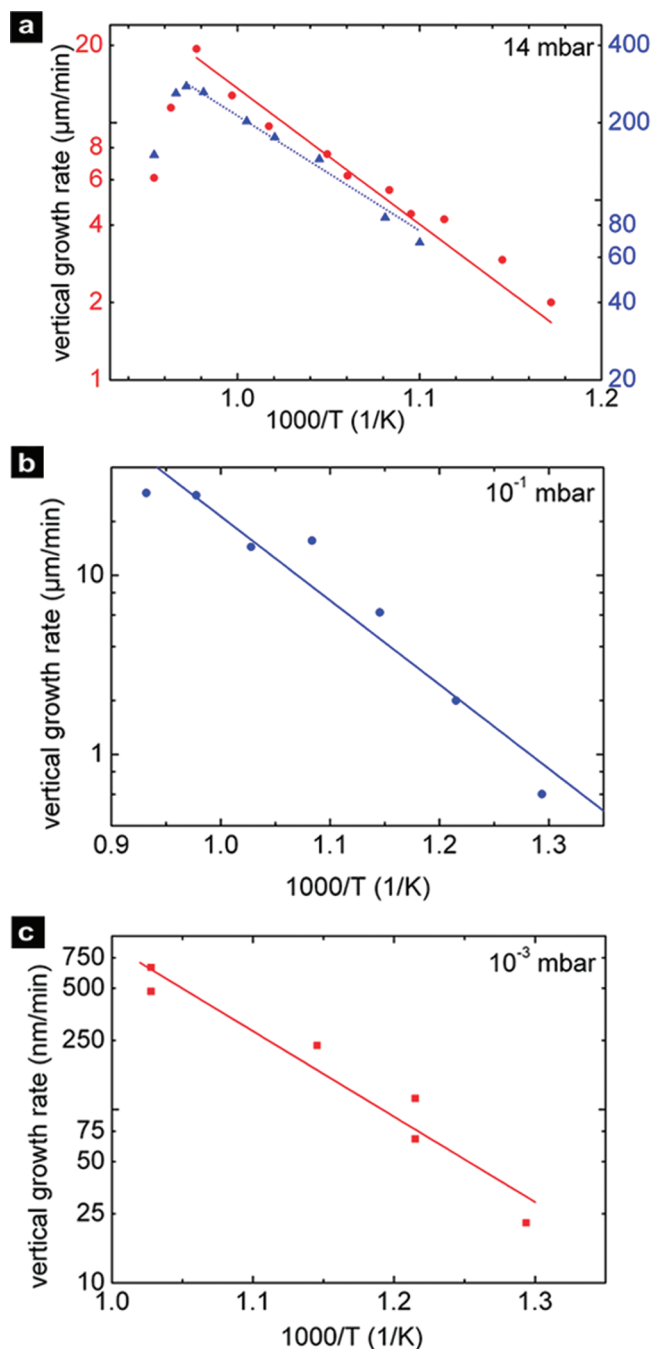$$\Delta E = E_1 - E_{-1} + E_2 \qquad (6)$$

Figure 4. (a) Arrhenius plots for CNT growth rates for atmospheric pressure (●) hot-walled furnace growth and (▲) cold-walled direct heating method from an Fe−Al$_2$O$_3$ catalyst in Ar/H$_2$/C$_2$H$_2$ (14 mbar partial pressure C$_2$H$_2$). The activation energies are calculated from the slope of the linear fit to the data, (●) $\Delta E = 0.95 \pm 0.04$ eV, (▲) $\Delta E = 0.92 \pm 0.04$ eV. (b) Arrhenius plot at a pressure of 15 mbar in a H$_2$/C$_2$H$_2$ mixture (0.37 mbar partial pressure C$_2$H$_2$), $\Delta E = 0.93 \pm 0.1$ eV. The catalyst was heated in H$_2$ before C$_2$H$_2$ was fed into the system. (c) Arrhenius plot at a pressure of 10^{-3} mbar C$_2$H$_2$, $\Delta E = 0.98 \pm 0.1$ eV. The C$_2$H$_2$ was undiluted during growth. The catalyst film was annealed in NH$_3$ prior to growth for 5 min.

This is dominated by E_2 as $E_1 \sim E_{-1}$. Thus, this mechanism accounts for both our observed pressure and temperature dependences. If the energy is released in the pre-equilibrium, the activation energy simplifies to $\Delta E = E_2$, but numerically there is not much difference be-
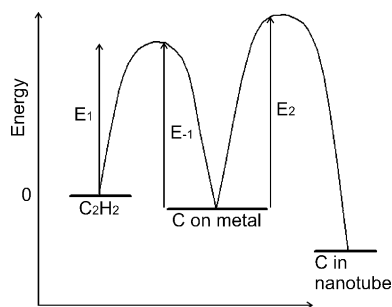
Figure 5. Energetics of the dissociation and diffusion steps. E_1 and E_{-1} are the energy barriers associated with dissociation rate constants k_1 and k_{-1}. E_2 is the energy barrier of diffusion on or in the metal. The overall activation energy is $E_1 - E_{-1} + E_2$.

tween this and eq 6. The experimentally observed activation energy corresponds to the carbon diffusion barrier E_2.

The values of E_1 and E_{-1} for the catalytic decomposition of acetylene on Fe surfaces into isolated atoms have previously been calculated; this dissociation reaction is exothermic and involves the formation of CH fragments as an intermediate step.[50] CH fragments can form *via* breaking either of the C—C bond of the C_2H_2 molecule or of CCH fragments, respectively. The energy barrier for the dissociation into C_1 species is of the order of 1 eV.[50] A similar calculation was also performed for the adsorption of acetylene on Ni surfaces.[29]

A diffusion-limited mechanism with predissociation accounts for many observations. First, if only solid-state diffusion mattered, this would not account for the huge dependence on catalyst characteristics. All nanoparticles of the same diameter would have the same catalyst efficiency, which is not true. The yield now depends *via K* on the density of active surface sites which dissociate the feedstock. Second, the feedstock gas matters. Different feedstocks will dissociate differently on the catalyst surface. Various groups have observed that nanotube forests grow taller on the outside of patterned shapes and that growth rates depend on gas flow conditions[6,22,23] and also on thermal treatment of the precursor.[51] These observations are not consistent with a solely solid-state diffusion-limited process.

A number of groups have previously measured the pressure dependence of growth rate over a limited pressure range and found it to peak.[34,52] These experiments used ethanol as feedstock. Molecular beam experiments showed that acetylene is the most active growth precursor,[53] and recently, two groups have shown that acetylene is the primary growth precursor in both hydrocarbon and alcohol feedstock conditions.[54,55] We would expect a monotonic pressure dependence over a large pressure range for the primary growth species, acetylene, as seen in Figure 3, but a more complex dependence for a secondary species like ethanol. For example, ethanol

could chemisorb dissociatively on the catalyst to form C_1 species in a pre-equilibrium step

$$C_2H_5OH \rightleftharpoons C_2H_{2\ ads} + H_2 + H_2O_{ads}$$
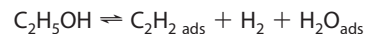
and then at higher pressures, the H_2O groups could block further adsorption or combine with carbon atoms and give a retarding step of CO desorption. In this case, the higher activation energies for the secondary species would correspond to their dissociation into acetylene.

We finally comment briefly on the growth deceleration step. For our catalyst preparation, we do not observe the abrupt growth termination found by some other groups with, for example, water-assisted growth from ethylene or other feedstocks.[18−20,34] We see a gradual decrease of catalyst activity. The decline is slightly stronger at high temperatures. Growth was sometimes also intentionally stopped because of a decline in nanotube quality as seen by an increased Raman D peak,[22] which could be due to an overcoating of the nanotubes by amorphous carbon. A key factor of SWNT growth is the kinetics of carbon supply. An oversupply of C causes the formation of multi-wall rather than single-walled nanotubes because excess C activity allows the nucleation of extra nanotube walls.[56] It can also cause the catalyst particle to be encapsulated with graphitic carbon.[21] In our work, we have counteracted this tendency by using low pressures or diluted acetylene for atmospheric pressure growth, and this might be a reason that sudden growth cessation is not observed.

In conclusion, we propose that the growth of vertically aligned carbon nanotube forests involves the dissociation of adsorbed C_2 species followed by a diffusion-limited growth. This is compatible with both the observed pressure and temperature dependence.

Supporting Information Available: Side view image sequences of Fe-catalyzed CNT forest growth. A ~5 × 15 mm^2 sized Fe(1 nm)/Al$_2$O$_3$(10 nm)/SiO$_2$(200 nm)/Si substrate is clamped between two copper posts and resistively heated to ~750 °C (pyrometer reading) in 200:500:10 sccm Ar/H$_2$/C$_2$H$_2$ in an atmospheric tube furnace. The total play time corresponds to 5 min (video 1) and 15 min (video 2) growth time. This material is available free of charge *via* the Internet at http://pubs.acs.org.

REFERENCES AND NOTES

1. Cassell, A. M.; Raymakers, J. A.; Kong, J.; Dai, H. Large Scale CVD Synthesis of Single-Walled Carbon Nanotubes. *J. Phys. Chem. B* **1999**, *103*, 6484–6492.
2. Wu, Z.; Chen, Z.; Du, X.; Logan, J. M.; Sippel, J.; Nikolou, M.; Kamaras, K.; Reynolds, J. R.; Tanner, D. B.; Hebard, A. F.; Rinzler, A. G. Transparent, Conductive Carbon Nanotube Films. *Science* **2004**, *305*, 1273–1276.
3. Li, Y.-L.; Kinloch, I. A.; Windle, A. H. Direct Spinning of Carbon Nanotube Fibers from Chemical Vapor Deposition Synthesis. *Science* **2004**, *304*, 276–278.

4. Nihei, M.; Kawabata, A.; Kondo, D.; Horibe, M.; Sato, S.; Awano, Y. Electrical Properties of Carbon Nanotube Bundles for Future *via* Interconnects. *Jpn. J. Appl. Phys.* **2005**, *44*, 1626–1628.

5. Huang, H.; Liu, C. H.; Wu, Y.; Fan, S. Aligned Carbon Nanotube Composite Films for Thermal Management. *Adv. Mater.* **2005**, *17*, 1652–1656.

6. Futaba, D. N.; Hata, K.; Yamada, T.; Hiraoka, T.; Hayamizu, Y.; Kakudate, Y.; Tanaike, O.; Hatori, H.; Yumura, M.; Iijima, S. Shape-Engineerable and Highly Densely Packed Single-Walled Carbon Nanotubes and Their Application as Super-Capacitor Electrodes. *Nat. Mater.* **2006**, *5*, 987–994.

7. Qu, L.; Dai, L.; Stone, M.; Xia, Z.; Wang, Z. L. Carbon Nanotube Arrays with Strong Shear Binding-On and Easy Normal Lifting-Off. *Science* **2008**, *322*, 238–242.

8. Robertson, J.; Zhong, G.; Telg, H.; Thomsen, C.; Warner, J. H.; Briggs, G. A. D.; Dettlaff-Weglikowska, U.; Roth, S. Growth and Characterization of High-Density Mats of Single-Walled Carbon Nanotubes for Interconnects. *Appl. Phys. Lett.* **2008**, *93*, 163111–163113.

9. Fan, S.; Chapline, M. G.; Franklin, N. R.; Tombler, T. W.; Cassell, A. M.; Dai, H. Self-Oriented Regular Arrays of Carbon Nanotubes and Their Field Emission Properties. *Science* **1999**, *283*, 512–514.

10. Li, X.; Cao, A.; Jung, Y. J.; Vajtai, R.; Ajayan, P. M. Bottom-Up Growth of Carbon Nanotube Multilayers: Unprecedented Growth. *Nano Lett.* **2005**, *5*, 1997–2000.

11. Hart, A. J.; Slocum, A. H. Rapid Growth and Flow-Mediated Nucleation of Millimeter-Scale Aligned Carbon Nanotube Structures from a Thin-Film Catalyst. *J. Phys. Chem. B* **2006**, *110*, 8250–8257.

12. Zhang, M.; Atkinson, K. R.; Baughman, R. H. Multifunctional Carbon Nanotube Yarns by Downsizing an Ancient Technology. *Science* **2004**, *306*, 1358–1361.

13. Murakami, Y.; Chiashi, S.; Miyauchi, Y.; Hu, M.; Ogura, M.; Okubo, T.; Maruyama, S. Growth of Vertically Aligned Single-Walled Carbon Nanotube Films on Quartz Substrates and Their Optical Anisotropy. *Chem. Phys. Lett.* **2004**, *385*, 298–303.

14. Hata, K.; Futaba, D. N.; Mizuno, K.; Namai, T.; Yumura, M.; Iijima, S. Water-Assisted Highly Efficient Synthesis of Impurity-Free Single-Walled Carbon Nanotubes. *Science* **2004**, *306*, 1362–1364.

15. Zhong, G. F.; Iwasaki, T.; Honda, K.; Furukawa, Y.; Ohdomari, I.; Kawarada, H. Low Temperature Synthesis of Extremely Dense, and Vertically Aligned Single-Walled Carbon Nanotubes. *Jpn. J. Appl. Phys.* **2005**, *44*, 1558–1561.

16. Zhang, L.; Tan, Y.; Resasco, D. E. Controlling the Growth of Vertically Oriented Single-Walled Carbon Nanotubes by Varying the Density of CoMo Catalyst Particles. *Chem. Phys. Lett.* **2006**, *422*, 198–203.

17. Xu, Y.-Q.; Flor, E.; Schmidt, H.; Smalley, R. E.; Hauge, R. H. Effects of Atomic Hydrogen and Active Carbon Species in 1 mm Vertically Aligned Single-Walled Carbon Nanotube Growth. *Appl. Phys. Lett.* **2006**, *89*, 123116.

18. Puretzky, A. A.; Geohegan, D. B.; Jesse, S.; Ivanov, I. N.; Eres, G. *In Situ* Measurements and Modeling of Carbon Nanotube Array Growth Kinetics during Chemical Vapor Deposition. *Appl. Phys. A* **2005**, *81*, 223–240.

19. Futaba, D. N.; Hata, K.; Yamada, T.; Mizuno, K.; Yumura, M.; Iijima, S. Kinetics of Water-Assisted Single-Walled Carbon Nanotube Synthesis Revealed by a Time-Evolution Analysis. *Phys. Rev. Lett.* **2005**, *95*, 056104.

20. Meshot, E. R.; Hart, A. J. Abrupt Self-Termination of Vertically Aligned Carbon Nanotube Growth. *Appl. Phys. Lett.* **2008**, *92*, 113107-3.

21. Yamada, T.; Maigne, A.; Yudasaka, M.; Mizuno, K.; Futaba, D. N.; Yumura, M.; Iijima, S.; Hata, K. Revealing the Secret of Water-Assisted Carbon Nanotube Synthesis by Microscopic Observation of the Interaction of Water on the Catalysts. *Nano Lett.* **2008**, *8*, 4288–4292.

22. Zhong, G. F.; Iwasaki, T.; Robertson, J.; Kawarada, H. Growth Kinetics of 0.5 cm Vertically Aligned Single-Walled Carbon Nanotubes. *J. Phys. Chem. B* **2007**, *111*, 1907–1910.

23. Xiang, R.; Yang, Z.; Zhang, Q.; Luo, G.; Qian, W.; Wei, F.; Kadowaki, M.; Einarsson, E.; Maruyama, S. Growth Deceleration of Vertically Aligned Carbon Nanotube Arrays: Catalyst Deactivation or Feedstock Diffusion Controlled. *J. Phys. Chem. C* **2008**, *112*, 4892–4896.

24. Baker, R. T. K.; Harris, P. S.; Thomas, R. B.; Waite, R. J. Formation of Filamentous Carbon from Iron, Cobalt and Chromium Catalyzed Decomposition of Acetylene. *J. Catal.* **1973**, *30*, 86–95.

25. Rostrup-Nielsen, J.; Trimm, D. L. Mechanisms of Carbon Formation on Nickel-Containing Catalysts. *J. Catal.* **1977**, *48*, 155–165.

26. Klinke, C; B, J.-M.; Kern, K. Thermodynamic Calculations on the Catalytic Growth of Multiwall Carbon Nanotubes. *Phys. Rev. B* **2005**, *71*, 035403.

27. Chhowalla, M.; Teo, K. B. K.; Ducati, C.; Rupesinghe, N. L.; Amaratunga, G. A. J.; Ferrari, A. C.; Roy, D.; Robertson, J.; Milne, W. I. Growth Process Conditions of Vertically Aligned Carbon Nanotubes Using Plasma Enhanced Chemical Vapor Deposition. *J. Appl. Phys.* **2001**, *90*, 5308–5317.

28. Hofmann, S.; Ducati, C.; Robertson, J.; Kleinsorge, B. Low-Temperature Growth of Carbon Nanotubes by Plasma-Enhanced Chemical Vapor Deposition. *Appl. Phys. Lett.* **2003**, *83*, 135–137.

29. Hofmann, S. C., G.; Ferrari, A. C.; Payne, M. C.; Robertson, J. Surface Diffusion: The Low Activation Energy Path for Nanotube Growth. *Phys. Rev. Lett.* **2005**, *95*, 036101.

30. Raty, J.-Y.; Gygi, F.; Galli, G. Growth of Carbon Nanotubes on Metal Nanoparticles: A Microscopic Mechanism from *Ab Initio* Molecular Dynamics Simulations. *Phys. Rev. Lett.* **2005**, *95*, 096103.

31. Liu, K.; Jiang, K.; Feng, C.; Chen, Z.; Fan, S. A Growth Mark Method for Studying Growth Mechanism of Carbon Nanotube Arrays. *Carbon* **2005**, *43*, 2850–2856.

32. Gunjishima, I.; Inoue, T.; Okamoto, A. *In Situ* Optical Imaging of Carbon Nanotube Growth. *Jpn. J. Appl. Phys.* **2007**, *46*, 3149–3151.

33. Mattevi, C.; Wirth, C. T.; Hofmann, S.; Blume, R.; Cantoro, M.; Ducati, C.; Cepek, C.; Knop-Gericke, A.; Milne, S.; Castellarin-Cudia, C.; Dolafi, S.; Goldoni, A.; Schloegl, R.; Robertson, J. *In-Situ* X-ray Photoelectron Spectroscopy Study of Catalyst-Support Interactions and Growth of Carbon Nanotube Forests. *J. Phys. Chem. C* **2008**, *112*, 12207–12213.

34. Einarsson, E.; Murakami, Y.; Kadowaki, M.; Maruyama, S. Growth Dynamics of Vertically Aligned Single-Walled Carbon Nanotubes from *In Situ* Measurements. *Carbon* **2008**, *46*, 923–930.

35. Geohegan, D. B.; Puretzky, A. A.; Ivanov, I. N.; Jesse, S.; Eres, G.; Howe, J. Y. *In Situ* Growth Rate Measurements and Length Control during Chemical Vapor Deposition of Vertically Aligned Multiwall Carbon Nanotubes. *Appl. Phys. Lett.* **2003**, *83*, 1851–1853.

36. Yasuda, S.; Futaba, D. N.; Yumura, M.; Iijima, S.; Hata, K. Diagnostics and Growth Control of Single-Walled Carbon Nanotube Forests Using a Telecentric Optical System for *In Situ* Height Monitoring. *Appl. Phys. Lett.* **2008**, *93*, 143115.

37. Cantoro, M.; Hofmann, S.; Pisana, S.; Scardaci, V.; Parvez, A.; Ducati, C.; Ferrari, A. C.; Blackburn, A. M.; Wang, K.-Y.; Robertson, J. Catalytic Chemical Vapor Deposition of Single-Wall Carbon Nanotubes at Low Temperatures. *Nano Lett.* **2006**, *6*, 1107–1112.

38. Warner, J. H.; Schaffel, F.; Zhong, G. F.; Rummeli, M. H.; Buchner, B.; Robertson, J.; Briggs, G. A. D. Investigating the Diameter-Dependent Stability of Single-Walled Carbon Nanotubes. *ACS Nano* **2009**, *3*, 1557–1563.

39. Hofmann, S.; Sharma, R.; Ducati, C.; Du, G.; Mattevi, C.; Cepek, C.; Cantoro, M.; Pisana, S.; Parvez, A.; Cervantes-Sodi, F.; Ferrari, A. C.; Dunin-Borkowski, R.; Lizzit, S.; Petaccia, L.; Goldoni, A.; Robertson, J. *In Situ* Observations of Catalyst Dynamics during Surface-Bound Carbon Nanotube Nucleation. *Nano Lett.* **2007**, *7*, 602–608.

40. Hofmann, S.; Cantoro, M.; Kleinsorge, B.; Casiraghi, C.; Parvez, A.; Robertson, J.; Ducati, C. Effects of Catalyst Film Thickness on Plasma-Enhanced Carbon Nanotube Growth. *J. Appl. Phys.* **2005**, *98*, 034308-8.

41. Cantoro, M.; Hofmann, S.; Mattevi, C.; Pisana, S.; Parvez, A.; Fasoli, A.; Ducati, C.; Scardaci, V.; Ferrari, A. C.; Robertson, J. Plasma Restructuring of Catalysts for Chemical Vapor Deposition of Carbon Nanotubes. *J. Appl. Phys.* **2009**, *105*, 064304.

42. Amama, P. B.; Pint, C. L.; McJilton, L.; Kim, S. M.; Stach, E. A.; Murray, P. T.; Hauge, R. H.; Maruyama, B. Role of Water in Super Growth of Single-Walled Carbon Nanotube Carpets. *Nano Lett.* **2009**, *9*, 44–49.

43. Smith, R. P. the Diffusivity and Solubility of Carbon in α-Iron. *Trans. Metall. Soc. AIME* **1962**, *224*, 105–111.

44. Vinten, P.; Lefebvre, J.; Finnie, P. Kinetic Critical Temperature and Optimized Chemical Vapor Deposition Growth of Carbon Nanotubes. *Chem. Phys. Lett.* **2009**, *469*, 293–297.

45. Zhu, L.; Xu, J.; Xiao, F.; Jiang, H.; Hess, D. W.; Wong, C. P. the Growth of Carbon Nanotube Stacks in the Kinetics-Controlled Regime. *Carbon* **2007**, *45*, 344–348.

46. Lee, Y. T.; Park, J.; Choi, Y. S.; Ryu, H.; Lee, H. J. Temperature-Dependent Growth of Vertically Aligned Carbon Nanotubes in the Range 800−1100 °C. *J. Phys. Chem. B* **2002**, *106*, 7614–7618.

47. Kim, K.-E.; Kim, K.-J.; Jung, W. S.; Bae, S. Y.; Park, J.; Choi, J.; Choo, J. Investigation on the Temperature-Dependent Growth Rate of Carbon Nanotubes Using Chemical Vapor Deposition of Ferrocene and Acetylene. *Chem. Phys. Lett.* **2005**, *401*, 459–464.

48. Noda, S.; Hasegawa, K.; Sugime, H.; Kakehi, K.; Zhang, Z. Y.; Maruyama, S.; Yamaguchi, Y. Millimeter-Thick Single-Walled Carbon Nanotube Forests: Hidden Role of Catalyst Support. *Jpn. J. App. Phys.* **2007**, *46*, L399–L401.

49. Pirard, S. L.; Douven, S.; Bossuot, C.; Heyen, G.; Pirard, J.-P. A Kinetic Study of Multi-Walled Carbon Nanotube Synthesis by Catalytic Chemical Vapor Deposition Using a Fe-Co/Al2O3 Catalyst. *Carbon* **2007**, *45*, 1167–1175.

50. Lee, G.-D.; Han, S.; Yu, J.; Ihm, J. Catalytic Decomposition of Acetylene on Fe(001): A First-Principles Study. *Phys. Rev. B* **2002**, *66*, 081403.

51. Meshot, E. R.; Plata, D. e. L.; Tawfick, S.; Zhang, Y.; Verploegen, E. A.; Hart, A. J. Engineering Vertically Aligned Carbon Nanotube Growth by Decoupled Thermal Treatment of Precursor and Catalyst. *ACS Nano* **2009**, *3*, 2477–2486.

52. Picher, M.; Anglaret, E.; Arenal, R.; Jourdain, V. Self-Deactivation of Single-Walled Carbon Nanotube Growth Studied by *In Situ* Raman Measurements. *Nano Lett.* **2009**, *9*, 542–547.

53. Eres, G.; Kinkhabwala, A. A.; Cui, H.; Geohegan, D. B.; Puretzky, A. A.; Lowndes, D. H. Molecular Beam-Controlled Nucleation and Growth of Vertically Aligned Single-Wall Carbon Nanotube Arrays. *J. Phys. Chem. B* **2005**, *109*, 16684–16694.

54. Zhong, G.; Hofmann, S.; Yan, F.; Telg, H.; Warner, J. H.; Eder, D.; Thomsen, C.; Milne, W. I.; Robertson, J. Acetylene: A Key Growth Precursor for Single-Walled Carbon Nanotube Forests. *J. Phys. Chem. C* **2009**, *113*, 17321–17325.

55. Xiang, R.; Einarsson, E.; Okawa, J.; Miyauchi, Y.; Maruyama, S. Acetylene-Accelerated Alcohol Catalytic Chemical Vapor Deposition Growth of Vertically Aligned Single-Walled Carbon Nanotubes. *J. Phys. Chem. C* **2009**, *113*, 7511–7515.

56. Wood, R. F.; Pannala, S.; Wells, J. C.; Puretzky, A. A.; Geohegan, D. B. Simple Model of the Interrelation between Single- And Multiwall Carbon Nanotube Growth Rates for the CVD Process. *Phys. Rev. B* **2007**, *75*, 235446.